THE AMERICAN SOCIETY OF MECHANICAL ENGINEERS
345 E. 47 St., New York, N.Y. 10017

82-GT-92

The Effect of Inlet Distortion on the Performance Characteristics of a Centrifugal Compressor

I. Ariga
Professor

N. Kasai
Postgraduate Student

S. Masuda
Associate Professor

Faculty of Science and Technology, Keio University, Yokohama, Japan

Y. Watanabe
Power Plant Overhaul Center, Japan Air Lines, Tokyo, Japan

I. Watanabe
Professor, Faculty of Engineering, Kanto-Gakuin University, Yokohama, Japan
Mem. ASME

The present paper concerns itself with the effects of total pressure (and thus velocity) distortion on performance characteristics and surge margin of centrifugal compressors. Both radial and circumferential distortions were investigated. The performance tests as well as the velocity measurements within the impeller passages were carried out with a low speed compressor test rig with the inlet honeycomb as the distortion generators and compared with the case of "no distortion" as a datum. The results indicated that the inlet distortion exerted unfavorable influences on the efficiency and the surge margin of the given compressor, though the influence of the radial distortion was much stronger than that of the circumferential one. Various distortion indices were further examined in order to correlate the performance to the inlet distortion.

NOMENCLATURE

C	absolute velocity [m/s]
H	total head [m]
Δh_{in}	shock loss at the impeller
h	length along blade height
h_t	distance from hub to shroud along quasi-orthogonal line
i	incidence angle [°]
l_1	curvilinear coordinate measured along shroud surface
l_{1-2}	total length of impeller measured along shroud surface
l_{inc}	total length of inducer
m	mass flow rate [kg/s]
N	rotational speed [rpm]
N_0	corrected speed ($=N\sqrt{T_0/T_a}$) [rpm]
P	pressure [Pa]
R	gas constant
T	temperature [K]
u	peripheral speed [m/s]
W	relative velocity [m/s[
β	inducer inlet angle [°]
η_{imp}	impeller efficiency

$$= \frac{\frac{\kappa}{\kappa-1} RT_1\left\{\left(\frac{P_{t1}}{P_{t2}}\right)^{\frac{\kappa-1}{\kappa}} - 1\right\}}{\mu u_2^2}$$

θ	circumferential location [°]
ϕ	flow coefficient (c_{2r}/u_2)
μ	slip factor
κ	ratio of specific heats

SUBSCRIPTS

0	standard condition
1	impeller inlet condition
2	impeller outlet condition
a	atmospheric condition
m	axial component
m*	through flow component
r	radial component
s	static
t	total

Contributed by the Gas Turbine Division of the ASME.

u peripheral component

s surge point

SUPERSCRIPT

- mass average

INTRODUCTION

In recent years, centrifugal compressors are increasingly utilized for various purposes, and the spatial restrictions become inherent with growing width of applications. In consequence, the flow nonuniformity is frequently generated at the impeller inlet.

This is generally known as "inlet distortion" which is divided mainly into "radial distrotion" and "circumferential distortion". The former one is further subdivided into "tip distortion" and "hub distortion" corresponding to the regions where the total pressure defect exists near a hub or a shroud side.

These may actually occur in the following cases:

1) Hub distortion -- axisymmetric obstacles at a center portion of an inlet, such as a tachometer pick up, a hub cover etc. or axisymmetric boundary layers of a return channel of multi-stage compressor.
2) Tip distortion -- axisymmetric boundary layers of an inlet duct or a return channel or axisymmetric obstacles such as an orifice plate.
3) Circumferential distortion -- non-axisymmetric obstacles such as struts or a bending duct.

With regard to an axial compressor, the effect of inlet distortions on its performance characteristics has been widely investigated, and it has been reported that the compressor performance was deteriorated due to the inlet distortions and at the same time the flow range became narrower. Distortion indices which may be correlated to the compressor performance have also been variously discussed as to axial compressors, an many proposals have been made.

Only a few data about the inlet distortions of centrifugal compressors are available up to now [1], [2], although the nonuniformity of inlet flow appears frequently.

In this paper, total pressure distortions are investigated, where the velocity is nonuniform and the static pressure is uniform at the inlet. Three kinds of distorted velocity profiles, including two radial distortions and one circumferential distortion together with the undistorted profile, are artificially given at the impeller inlet.

In the following section, the results of the performance tests as well as the velocity measurements within the impeller passage are reported, and the effects of inlet distortion on performances and flow range are clarified. The distortion index is also discussed.

EXPERIMENTAL EQUIPMENTS AND METHODS

The test compressor configuration is shown in Fig. 1. Since its details were given in the reference

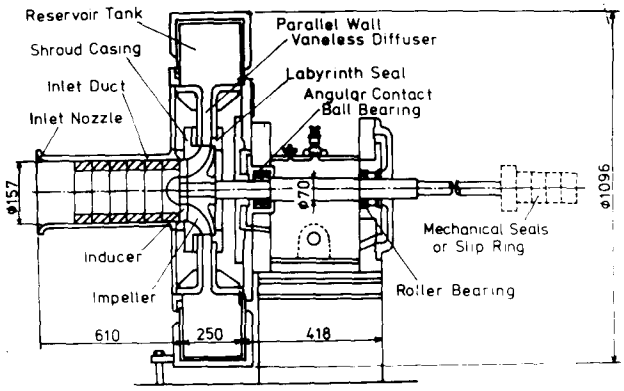

Fig. 1 Compressor configulation

Table. 1 Compressor specifications

Shape of Blade	Radial Straight
Dia. of Impeller Outlet	270mm
Inner Dia. of Impeller Inlet	81 mm
Outer Dia. of Impeller Inlet	157mm
Blade Height at Impeller Outlet	16.9mm
Number of Blades	12
Blade Thickness	3mm
Rotation Speed at Design Point	6000rpm
Flow Coeffcient at Design Point C_{2r}/U_2	0.4
Static Pressure Ratio at Design Point	1.04

Table. 2 Kinds of distortion

DISTORTION PATTERN	BLOCKED AREA RATIO	DISTORTION GENERATOR
NO DIST (No Distortion)	0	No Honeycomb
HUB DIST (Hub Distortion)	1/2	Cylindrical Honeycomb at the Hub Side
TIP DIST (Tip Distortion)	1/2	Cylindrical Honeycomb at the Shroud Side
CIRC DIST (Circumferential Distortion)	1/2	Fan-Shaped Honeycomb

[3], only the main points are to be repeated in the following. This compressor is driven by an eddy-current motor and its rotational speed can be changed from standstill to 6,300 rpm continuously.

The pressure signals from the rotating impeller is lead through the pipes buried in the shaft to the sealed channels consisted of four mechanical seals, then onto a stationary manometer. The electrical signals of the rotating hot-wire probe are transmitted through a five poles slip ring unit to a constant temperature anemometer.

The compressor specifications are illustrated in Table 1. An impeller with straight blades employed in the present study has a diffusion ratio, C_{2r}/C_{1m}, of 1.0. An inducer has a parabolic camber line. The inducer is designed such that shockless inlet condition along the span at an inducer leading edge is attained at the design point.

The experiments were carried out in the ranges of the corrected speeds N_0 = 6,000, 5,000, 4,000 rpm and the flow coefficients ϕ = 0.3, 0.4, 0.5. Several kinds of distortion are used in the experiments, as shown in Table 2.

The test cross sections were at the locations of 5mm upstream of the inducer leading edge and downstream of the impeller, respectively. The measurement points in those sections were selected at twelve sites for the inlet and nine sites for the outlet between the hub and shroud sides. Especially in the case of CIRC DIST, six circumferential locations were adopted as shown in Fig. 2. A kiel probe and three holes yaw probe were used for the measurements of time averaged total pressure and flow angle.

Concerning the relative flow patterns in the impeller, two probes, a three holes yaw probe for the time averaged value and a hot-wire probe for the time dependent value were traversed in the meridional direction at the mid-passage.

The static pressure taps were placed along the shroud casing from the inlet to the outlet. To detect the surge phenomenon, pressure transducer was installed on the shroud casing of the inducer throat.

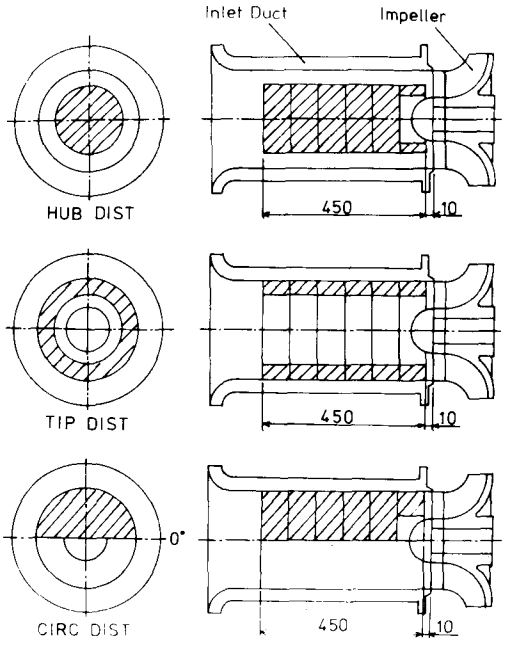

Fig. 2 Setting location of distortion generater

INLET CONDITIONS

The typical inlet distortion patterns of the radial distortions for the corrected speed N_0 = 6,000 rpm are given in Fig. 3, 4, and 5 for three values of flow coefficient including the design value of ϕ = 0.4. Fig. 3 shows the distributions of axial velocities measured at the location of 5mm upstream of the impeller inlet. Their nonuniformities increase with increasing flow rate because the pressure loss generated by the distortion generator is proportional to the square of the velocity. Fig. 4 shows the relative velocity distribution at the inlet section. While the detects of the axial velocity for the hub and the tip distortions are nearly equal as seen in the previous figure, those of the relative velocity become somewhat greater for the hub distortion than for the tip distortion due to the effect of the circumferential velocity. The corresponding incidence angle distributions are shown in Fig. 5. For all three inlet conditions, the average values vary from negative for the larger flow rate to positive for the smaller flow rate, being nearly zero for the design condition. The local portion of the negative incidence where the inflow attains toward the suction side of the inducer blade, exists in the region of higher axial velocities, i.e. in the shroud region for the hub distortion and in the hub region for the tip distortion. The appearance of such negative incidences on the blading may be related to the unfavorable operating conditions.

The circumferential distributions of the axial and the relative velocities for the circumferential distortion are shown in Fig. 6, in which the mass averaged values in the hub-shroud section are plotted, including in the next figure. As shown in the figure, the honeycomb is placed at the circumferential location between 0° and 180°. The difference between the maximum and the minimum velocities are again remarkable with increasing flow rate. In Fig. 7, corresponding incidence angle distributions are shown, where the negative incidence angle can be seen in the circumferential range without the blockage on the flow due to the existence of honeycomb.

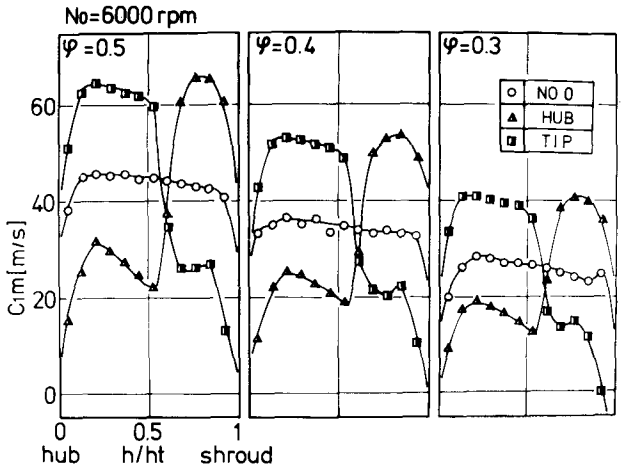

Fig. 3 Axial velocity distributions for no/radial distortions at the inducer inlet (No=6000rpm, φ=0.50, 0.40, 0.30)

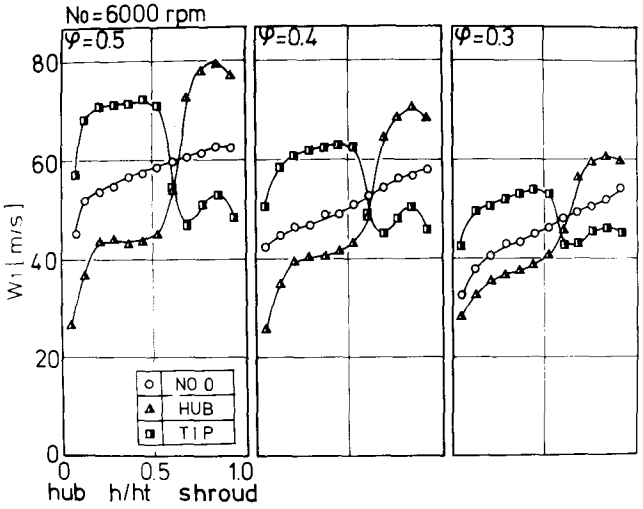

Fig. 4 Relative velocity distributions for no/radial distortions at the inducer inlet (No=6000rpm, ϕ=0.50 0.40, 0.30)

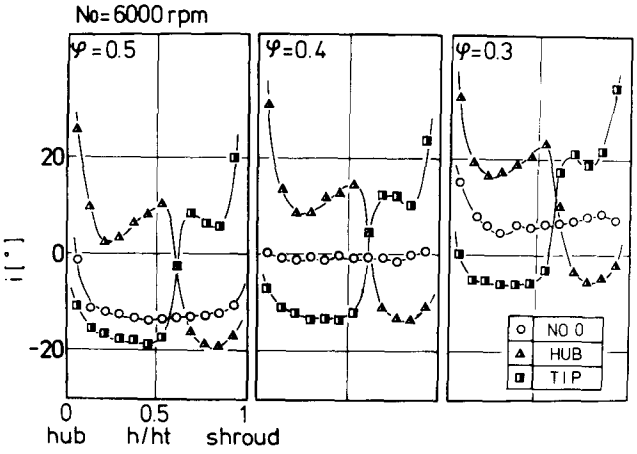

Fig. 5 Incidence angle distortions for no/radial distortions at the inducer inlet (No=6000rpm, ϕ=0.50, 0.40, 0.30)

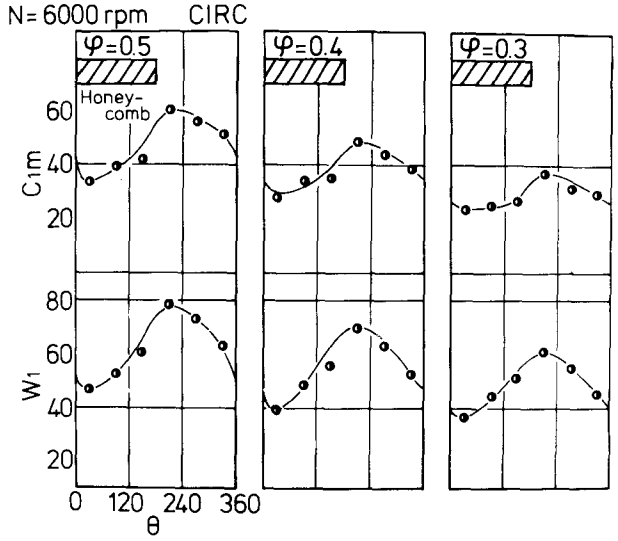

Fig. 6 Axial and relative velocity distributions for circumferential distortion at the impeller inlet (No=6000rpm, ϕ=0.50, 0.40, 0.30)

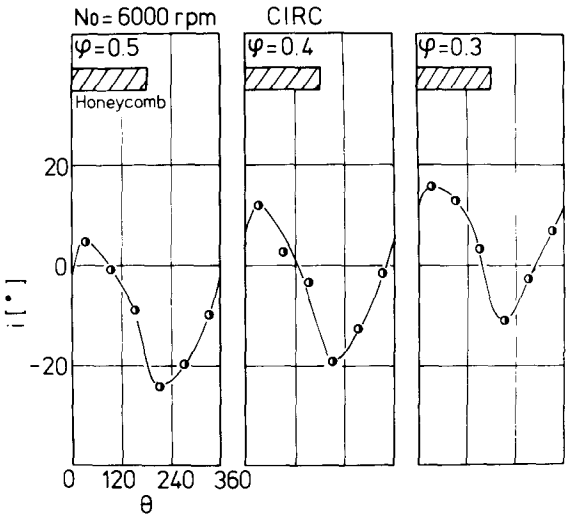

Fig. 7 Incidence angle distributions for circumferential distortion at the impeller inlet (No=6000rpm, ϕ=0.50, 0.40, 0.30)

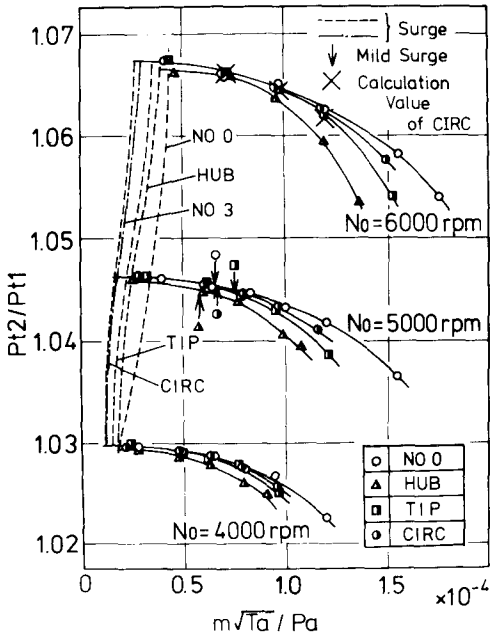

Fig. 8 Comparison of performance curves with various distortions

PERFORMANCE CHARACTERISTICS

In Fig. 8, the total pressure ratios of the impeller are plotted against the mass flow function for the three distortions as well as the undistorted cases. The highest pressure ratio is obtained in case of NO DIST (no distortion) and it falls gradually in the order of CIRC DIST (circumferential distortion), TIP DIST (tip distortion) and HUB DIST (hub distortion). This degeneration becomes more remarkable when the mass flow function increases and there seems no effect of the inlet distortion at the smallest mass flow function shown in the figure. These

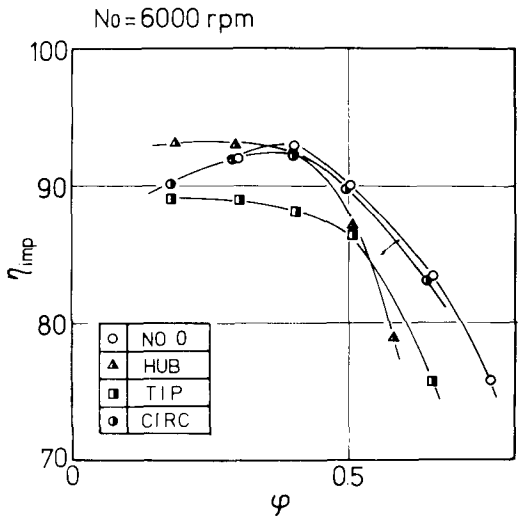

Fig. 9 Impeller efficiency

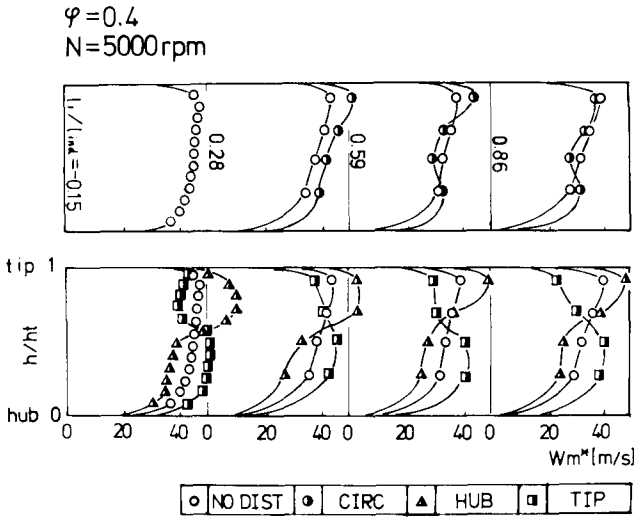

Fig. 10 The velocity profile within the inducer (No=5000rpm, ϕ=0.40)

tendencies are recognized equally for all three rotational speeds, though the effect of distortion slightly grows as the rotational speed increases.

The violent surge lines are also shown in the same figure. Unlike the total pressure ratio, the violent surge limit is the highest for the NO DIST and it moves to the lower flow rate in the order of HUB DIST, TIP DIST and CIRC DIST. Although these results reflect the effect of distortion itself, we must not fail to notice an influence of duct resistance associated with the inlet honeycomb, too. Mild surge limit at corrected speed N_0 = 5,000 rpm is shown by arrow marks in Fig. 8. The tendency of mild surge limits differs from that of violent surge. On these subjects, we will discuss later.

Fig. 9 shows the variation of the impeller efficiency for N_0 = 6,000 rpm. In accordance with the total pressure ratio, CIRC DIST has the smallest influence, the peak efficiency and the corresponding flow coefficient as well as the off-design variations being the same as those for NO DIST. The radial distortions, on the other hand, have remarkable influences on the impeller efficiencies. TIP DIST shows the lowest efficiency in almost all the range of flow coefficients tested. The more striking features are seen in the efficiency curve for HUB DIST, which is characterized by the efficiency higher than that for NO DIST at the small flow rate (ϕ<0.4) and the steep decrease at the large flow rate.

MEAN FLOW PATTERN WITHIN THE IMPELLER PASSAGE

In order to examine the behavior of the distorted velocity profile within the impeller passage, the time averaged velocities were measured by the three hole yaw probe mounted on the rotating impeller for ϕ = 0.40 and N_0 = 5,000 rpm. The typical results obtained within the inducer are given in Fig. 10 together with the velocity profile just upstream of the inducer. In the case of the radial distortions, the velocity profile given at the inlet is maintained to the downstream end of the inducer. Since the circumferential distortion is seen from the rotating

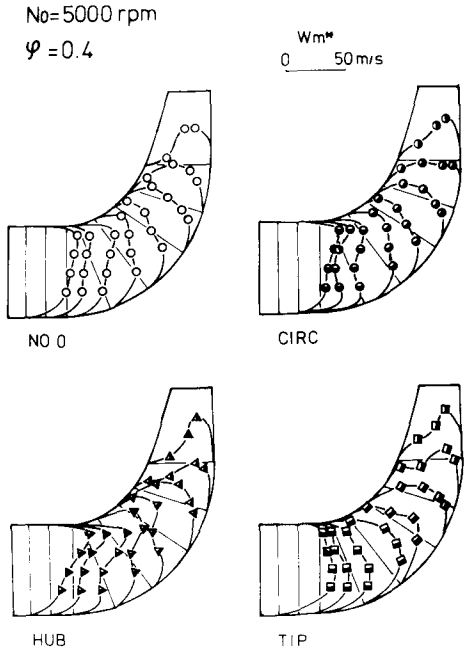

Fig. 11 The velocity profile within the impeller passage (No=5000rpm, ϕ=0.40)

frame as the periodic flow, the time averaged velocity profile within the inducer is apparently the same as that of NO DIST.

Fig. 11 shows the development of velocity profile further downstream within the impeller passage. In all cases, the velocity profiles at the second half of the impeller become nearly the same, with the velocity peak being near the hub side. Without distortion, the peak exists near the shroud side at the first half of the impeller and it moves to the hub side in the downstream direction. These tendencies are intensified in case of HUB DIST, where the initial velocity near the shroud side is artificially increased. In the case of TIP DIST, the velocity profile remains almostly unchanged, with the velocity peak lying always near the hub side. The flow

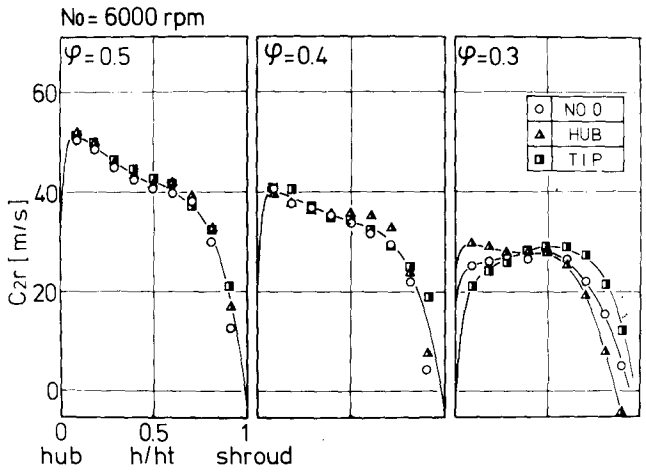

Fig. 12 Radial velocity distributions for no/radial distortions at the impeller outlet (No=6000rpm, ϕ=0.50, 0.40, 0.30)

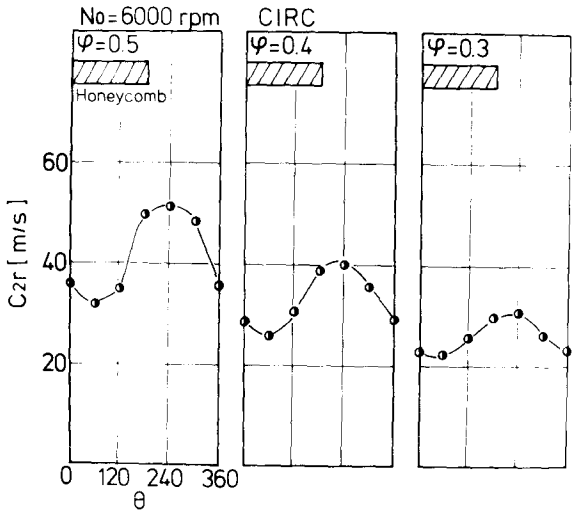

Fig. 13 Radial velocity distribution of circumferential distortion at the impeller outlet (No=6000rpm, ϕ=0.50, 0.40, 0.30)

development of CIRC DIST is hardly distinguishable from that of NO DIST in the time mean manner.

OUTLET VELOCITY PROFILE

The radial component of the absolute velocities at the location of 5mm downstream of the impeller outlet are given in Figs. 12 and 13 for the radial and the circumferential distortions, respectively. As seen in Fig. 12, the outlet velocity profiles of the radial distortions leave no traces of the inlet conditions except for the smallest flow rate (ϕ = 0.30). One of the interesting results is seen in Fig. 12 for ϕ = 0.30, where the effect of inlet conditions is remarkable, though the velocity profiles are entirely different from those given at the inlet. Since the complete measurement of flow development through the whole passage of the impeller was performed only for ϕ = 0.40, it is difficult to clear up the causes, but the remarkable difference of the impeller efficiency at small flow rates shown in Fig. 9 may be closely related to the distinct feature of the outlet velocity profile.

The outlet velocity distributions for the circumferential distortion shown in Fig. 13 exhibit another interesting result. In contrast to the radial distortions, the traces of the inlet distortion are clearly found at the outlet. It is also worth noticing that the defect of the outlet velocity exists just at the same angular position as given at the inlet, in spite of the rotating impeller lying between them (cf. Fig. 6).

TIME DEPENDENT MEASUREMENT OF CIRC DIST

As explained earlier, the time averaged measurements in the impeller passage for the circumferential distortions exhibit no appreciable difference as compared with the undistorted case. The results of the time dependent measurements of the through flow velocity within the impeller channel Wm* are shown in Fig. 14 together with the relative velocities W_1 and W_2 at the inlet and the outlet cross sections, respectively. Wm* was obtained using the rotating hot-wire probe fixed at the mid point of the channel cross section and one cycle of the time dependent signals was coverted into the function of angular positions measured from the fixed origin in the stationary frame. The velocity profiles within the impeller are well coincided with those at the inlet and the outlet, which means that the flow associated with the circumferential distortion is spatial within the entire flow region including the rotating impeller if it is observed from the stationary frame of reference. The whole length of an impeller channel accepts the periodic variation of flow rates simultaneously and one channel of the impeller experiences the small and large flow rates alternatively as it rotates passing through the angular regions of low and high velocities.

Fig. 15 shows the static pressure distribution along the radial lines on the shroud casing. At the circumferential locations θ = 150° and 210°, which correspond to the region near the minimum velocity, the static pressure once decreases to the minimum at the first quarter of the impeller and then increases. On the other hand, it increases monotonously in the region near maximum velocity, say at θ = 330°.

The two figures suggest the possibility of extending the idea of "parallel compressor" model, which was proposed by Doyle [4], Reid [5] and Roberts [6] for axial compressors, to centrifugal compressors with the circumferential distortions. In one period of time when a channel rotates through the region behind the honeycomb, it acts as if it were operating steadily at a point lying in the region of small flow rate on the undistorted performance map. In the rest of one cycle, the channel acts as if it were operating at another point lying in the region of larger flow rate.

On the basis of this model, the total pressure ratio for the circumferential distortion is estimated using the following relation;

$$Pr'(\phi) = \frac{\int_{\phi_{min}}^{\phi_{max}} Pr(\phi)\phi d\phi}{\phi(\phi_{max} - \phi_{min})} \qquad (1)$$

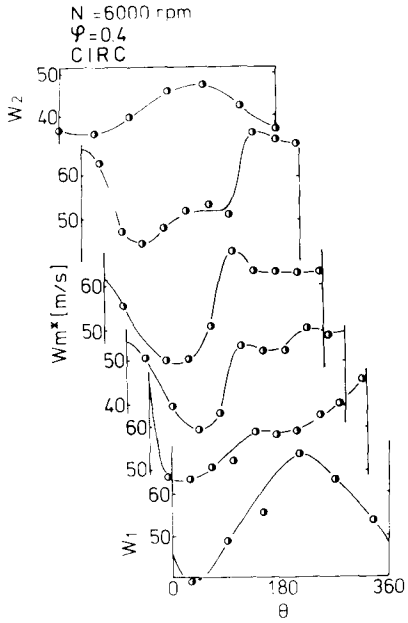

Fig. 14 Through flow velocity distribution within impeller channel by hot-wire, including relative velocity distribution at the impeller inlet and outlet (No=6000rpm, ϕ=0.40)

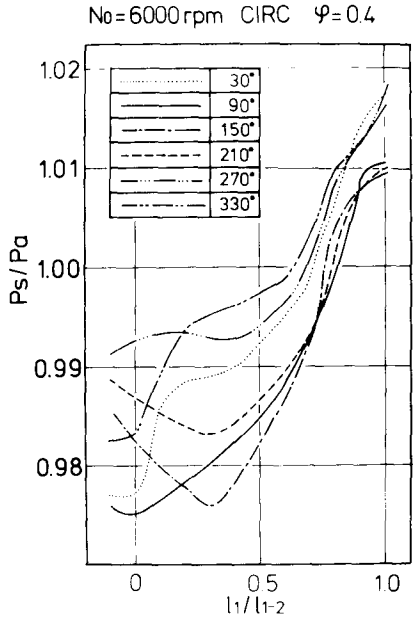

Fig. 15 Shroud surface static pressure distribution for circumferential distortion (No=6000rpm, ϕ=0.40)

where Pr and Pr' are the total pressure ratios for the undistorted condition and for the circumferential distortions, respectively and ϕ_{max} and ϕ_{min} are the maximum and the minimum values of the local flow coefficients for the circumferential distortion at a given mean flow coefficient. The calculated values are plotted in Fig. 8, which shows good correlation with the measured results, and supports the applicability of the "parallel compressor" model to centrifugal compressors with the circumferential distortions. It is also clear that the effect of circumferential distortions on performance characteristics is dependent not only on the pattern of distortion but also on the shape of the performance curve for undistorted conditions. As the first approximation, the total pressure ratio is improved or deteriorated by the circumferential distortions according to the sign of $dPr/d\phi$ of the undistorted curve at the mean operation point.

The direct application of this model to the radial distortions is impossible because the region of high and low velocities are not isolated in those cases but mixed within one channel of the impeller and it may cause the additional complexity such as loading distribution, secondary flows, leakage and so on.

DISTORTION INDEX

It is desirable to have a single parameter which correlates performance characteristics with the patterns of inlet distortions uniquely. Such a parameter is called "distortion index" and many proposals have been made on the distortion indices for axial compressors with the circumferential distortions as summarized in [7]. Since we are dealing with the centrifugal compressor with the radial and circumferential distortions together, we tried to find a new index which is applicable to these cases.

As stated before, some parts of the inducer blading have non-zero incidence angle, though it is equal to zero in the mean. Shock loss associated with it may be considered as one of the major factors causing the additional losses due to distortions of both types. So, we have tried to relate a new index with the shock loss of the inducer. O'neil et al. [8] suggested that the shock loss is proportional to the square of the relative peripheral velocity ΔW at the leading edge of the inducer. The distortion index may then be defined as

$$DI = \frac{\Delta h_{in}}{H_1} \tag{2}$$

where

$$\Delta h_{in} = \zeta_{in} \frac{\Delta W^2}{2g} \tag{3}$$

$$\Delta W = W_{1u} - W_{1m} \cdot \tan\beta \tag{4}$$

H_1 = inlet total head

Here the shock head coefficient is determined experimentally, and ζ_{in} = 0.6 from the present experiment.

Fig. 16 shows the relation between DI and ϕ for all cases of distortions tested.

Comparison with the total pressure ratio given in Fig. 16 indicates that DI is the suitable parameter for estimating the total pressure ratio with inlet distortions.

SURGE MARGIN

Surge regions are divided into "Mild surge" and "Violent surge". In the former case, pressure fluctuations detected only by a pressure transducer are still small, and in the latter case, the large flactuations are observed anywhere in the machine, accompanied with the vibration of a compressor.

Violent Surge

As already shown in Fig. 8, the violent surge margin is affected by the inlet distortions. It is well known, however, that a surge margin is also related to a flow resistance of an entire compressor passage, which varies with the distortion generators in the present cases. Hence, it was tried to investigate the effects of inlet distortion patterns, themselves, on the surge margin except for the differences of the resistance through the distortion generators.

Fig. 17 indicates the relation between the flow coefficients on the violent surge line and the inlet static pressure normalized by the atmospheric pressure at $\phi = 0.40$. The latter is related to the flow resistance through the honeycomb section. As references, the three additional undistorted conditions, NO. 1, NO. 2 and NO. 3 are included herein. They are generated by the one, two and three pieces of full shaped honeycomb of 75mm thick which are installed in series in the inlet pipe, respectively, and they can generate the uniform flows with different resistances. The performances for them were agreed almostly with that for NO. 0 as shown in Fig. 8.

The results of four kinds of undistorted conditions lie on a single straight line, which indicates that the resistance alone reduces the violent surge flow rate. The resistance of the three distored conditions are nearly equal those of NO. 1 and NO. 2, and these five results may be compared in order to examin the effect of distortion with the same level of resistance. It is clear from this comparison that the violent surge flow rate is reduced by CIRC DIST, increased by HUB DIST and unaffected by TIP DIST.

Mild Surge

Rodgers [9] proposed that a compressor stall, and consequently a mild surge, could be related with

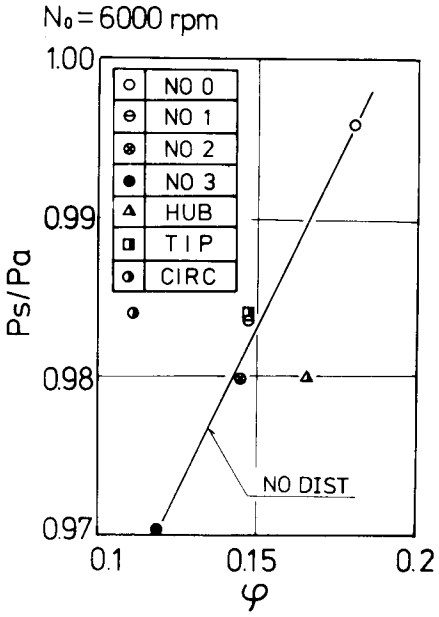

Fig. 17 Relation of static pressures upstream of the impeller inlet with flow coefficients at violent surge point (N0=6000rpm)

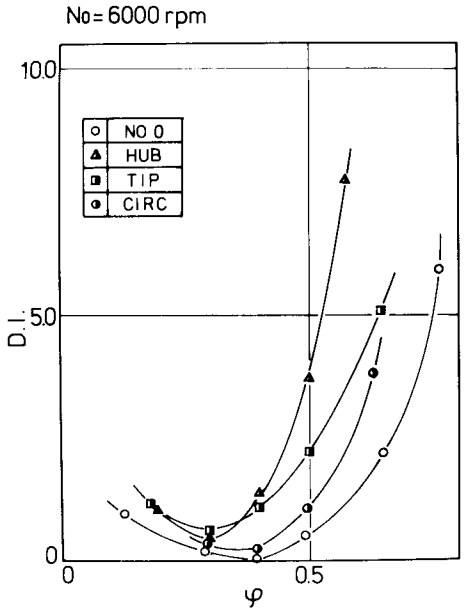

Fig. 16 Distortion index DI plotted against the flow coefficient for four distortions (N0=6000rpm)

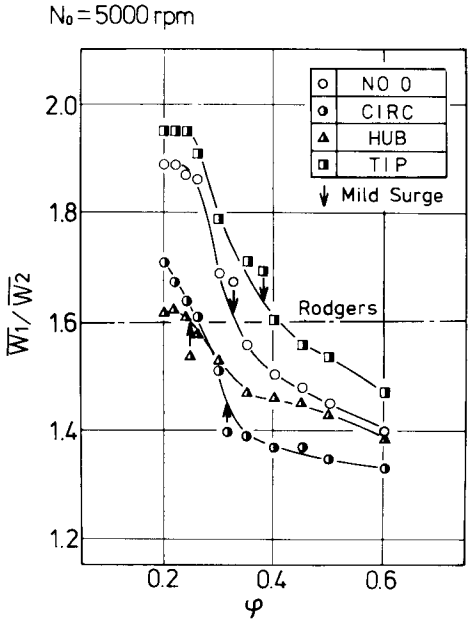

Fig. 18 Relation of mild surge points with ratio of inlet average relative velocity to outlet one

a diffusion factor defined as a ratio of inlet and outlet relative velocities (W_1/W_2), and gave $W_1/W_2 = 1.6$ as the criterion for occurrence of a mild surge. It is interesting to examine whether his criterion is applicable also to the distorted cases. In Fig. 18, the diffusion factors, which are evaluated from the mass flow average of relative velocities, are given as the functions of the flow coefficients and the mild surge limited are shown by the arrows.

It is clearly seen in this figure that mild surge of a radial distortion is well predicted by Rodgers' criterion, but it can not directly by applied to circumferential distortion.

CONCLUSION

In the present paper the authors experimentally investigated the effects of inlet total pressure distortion, i.e. radial and circumferential distortions on the performance characteristics and surge margin of a centrifugal compressor. Various distortion indices were also examined in order to correlate the performance to the inlet distortion.

The results are summarised as follows:

1) Compared with undistorted case, total pressure ratios fall in the order of circumferential, tip and hub distortions.

2) Distortion index DI, employing the shock loss of the inducer,

$$DI = \frac{\Delta h_{in}}{H_1}$$

is the suitable parameter for estimating the total pressure ratio with inlet distortions.

3) At the impeller outlet, the circumferential inlet distortion remains at the same circumferential location, while the effect of radial distortion almost disappears except for small flow rate.

4) "Parallel compressor" model can be applied to centrifugal compressors with circumferential distortions.

5) Violent surge is prompted by hub distortion and restrained by circumferential distortion, while it is unaffected by tip distortion if they are compared in the same level of duct resistance.

6) A mild surge limit of radial distortion is well predicted by Rodgers' criterion, while it is not directly applicable to circumferential distortion.

ACKNOWLEDGMENT

The authors wish to express their thanks to I. Ikeda, N. Ishikawa, H. Kousaka, T. Yoshida, K. Kunimatsu, H. Kurata, M. Uenoyama and A. Ookita.

This research was carried out partly with Grants in Aid for Scientific Research of the Ministry of Education in Japan in 1980 and also performed partially under the subcommittee RC-50 of the Japan Society of Mechanical Engineers.

REFERENCES

1. Лившич, С.И., "Аэродинамика Центробежных Компрессорных Машин," Машиностроение, 1966.

2. Benvenuti, E., Bonciani, L., Corradini, U., "Inlet Flow Distortions on Industrial Centrifugal Compressor Stages Experimental Investigations and Evaluation of Effects on Performance," AGARD Conference Preprint, NO. 282, Reference 4, 1980.

3. Mizuki, S., Ariga, I., and Watanabe, I., "Investigation Concerning the Blade Loading of Centrifugal Impellers." ASME Paper 74-GT-143, 1974.

4. Doyle, M.D.C., and Horlock, J.H., "Circumferential Asymmetry in Axial Flow Compressors," Journal of the Royal Aeronautical Society, Vol.70, 1966, pp. 956-957.

5. Reid, C., "The Response of Axial Flow Compressors to Intake Flow Distortion," ASME Paper 69-GT-29, 1969.

6. Roberts, F., Plourde, G.A., and Smakula. F., "Insights into Axial Compressor Response to Distortion," AIAA Paper NO. 68-595, 1968.

7. Graber, E.J.Jr., and Braithwaite, W.M., "Summary of Recent Investigations of Inlet Flow Distortion Effects on Engine Stability," AIAA Paper NO. 74-236, 1974.

8. O'neil, P.P., and Wickli, H.E., "Predicting Process Gas Performance of Centrifugal Compressors From Air Test Data," Journal of Engineering for Industry, Trans. ASME, Series B, Vol.84, 1962, pp. 248-264.

9. Rodgers, C., "Impeller Stalling as Influenced by Diffusion Limitations," Journal of Fluids Engineering, Trans. ASME, Series I, Vol.99, 1977, pp. 84-93.